The EMBO Journal Vol. 19 No. 20 pp. 5514–5524, 2000

She2p, a novel RNA-binding protein tethers *ASH1* mRNA to the Myo4p myosin motor via She3p

Florian Böhl, Claudia Kruse, Andrea Frank, Dunja Ferring and Ralf-Peter Jansen[1]

ZMBH, University of Heidelberg, Im Neuenheimer Feld 282, D-69120 Heidelberg, Germany

[1]Corresponding author
e-mail: r.jansen@mail.zmbh.uni-heidelberg.de

RNA localization is a widespread mechanism to achieve localized protein synthesis. In budding yeast, localization of *ASH1* mRNA controls daughter cell-specific accumulation of the transcriptional regulator Ash1p, which determines mating type switching. *ASH1* mRNA localization depends on four independently acting sequences ('zipcodes') within the mRNA. In addition, the class V myosin Myo4p and a set of She proteins with as yet unknown function are essential for *ASH1* localization. Here we show that She2p is a novel RNA-binding protein that binds specifically to *ASH1* mRNA *in vivo* and to *ASH1* RNA zipcodes *in vitro*. She2p can interact with She3 protein via She3p's C-terminus and becomes localized to the daughter cell tip upon *ASH1* expression. The N-terminal coiled-coil domain of She3p is required to form an RNA-independent complex with the heavy chain of the myosin motor protein Myo4p. She2p and She3p are the first examples of adapters for tethering a localized mRNA to the motor protein and might serve as prototypes for RNA–motor protein adapters.

Keywords: cytoskeleton/myosin/RNA localization/ *Saccharomyces cerevisiae*/yeast

Introduction

mRNA localization is a widespread mechanism by which cells generate asymmetry. It occurs in organisms as diverse as amoeba, yeast, plants, insects and vertebrates (for reviews see Bassell *et al*., 1999; Lasko, 1999; Mowry, 1999; Kiebler and DesGroseillers, 2000). Site-specific mRNA localization can be achieved by local protection, site-specific mRNA anchoring or mRNA transport (for an overview see Bashirullah *et al*., 1998).

RNA localization depends on signals within the mRNA as well as on proteins that recognize these signals. In the majority of cases, localization signals (also named zipcodes; Singer, 1993) reside in the 3′ untranslated region (3′UTR) of the mRNA. Only a few mRNAs have been reported with signals in the 5′UTR or in the coding region (Capri *et al*., 1997; Chartrand *et al*., 1999; Gonzalez *et al*., 1999; Thio *et al*., 2000). Proteins that recognize zipcodes have been isolated from various organisms (see Lasko, 1999; Mowry, 1999; Schnapp, 1999 for recent reviews). Most of them contain RNA-binding motifs like the double-stranded RNA-binding domain (Bycroft *et al*., 1995), the RNA recognition motif (RRM) domain (Query *et al*., 1989) or the hnRNP K homology (KH) domain (Adinolfi *et al*., 1999). In addition to such RNA-specific proteins, active transport of mRNAs requires a functional cytoskeleton and motor proteins that move along cytoskeletal filaments. Both actin-dependent myosin and microtubule-dependent kinesin motor proteins have been implicated in mRNA transport (Carson *et al*., 1997; Long *et al*., 1997; Takizawa *et al*., 1997). How the messenger ribonucleoprotein (mRNP) complex docks to the corresponding motor proteins is largely unknown but binding might require the function of adapter proteins that bridge between the mRNP proteins and the motors.

The only known actin-dependent motor protein with a specific role in mRNA localization is Myo4p, a class V myosin in *Saccharomyces cerevisiae* (Haarer *et al*., 1994; Long *et al*., 1997; Takizawa *et al*., 1997). Myo4p is essential for the localization of *ASH1* mRNA to daughter cells in yeast. *ASH1* encodes a transcriptional repressor that determines proper mating type switching by differentially regulating expression of the HO endonuclease (Bobola *et al*., 1996; Cosma *et al*., 1999). *ASH1* mRNA is expressed at the end of anaphase and subsequently localized to the tip of the maturing daughter cell (Long *et al*., 1997; Takizawa *et al*., 1997). Localization depends on signals in the coding region and 3′UTR of *ASH1* mRNA (Chartrand *et al*., 1999; Gonzalez *et al*., 1999). Five proteins (She1p–She5p) have been identified that are essential for *ASH1* mRNA localization (Jansen *et al*., 1996; Long *et al*., 1997). One of them, She1p, is identical to Myo4p. Whereas two of the She proteins, She4p and She5p/Bni1p, are required for diverse cellular processes (Wendland *et al*., 1996; Evangelista *et al*., 1997), She1p/Myo4p, She2p and She3p appear to be specific for mRNA transport. However, the function of She2p and She3p during localization has not yet been understood. It has previously been shown that She3p and Myo4p colocalize with RNP particles that contain *ASH1* RNA and that they can coprecipitate *ASH1* mRNA from cell extracts (Bertrand *et al*., 1998; Münchow *et al*., 1999; Takizawa and Vale, 2000). Both proteins appear to associate with *ASH1* RNP particles that have been observed to move from the mother to the daughter cell in live cells (Bertrand *et al*., 1998; Takizawa and Vale, 2000). However, it is not yet clear how the localization machinery recognizes the zipcode signals within *ASH1* RNA and which proteins tether the RNA to the motor protein.

In order to understand the molecular details of this tethering we investigated the binding of She2p, She3p, Myo4p and *ASH1* mRNA to each other *in vivo* and *in vitro*. Here we report that She2p binds *ASH1* directly via its zipcode elements and that She3p serves as a linker to connect She2p to the motor Myo4p. She2p binding of

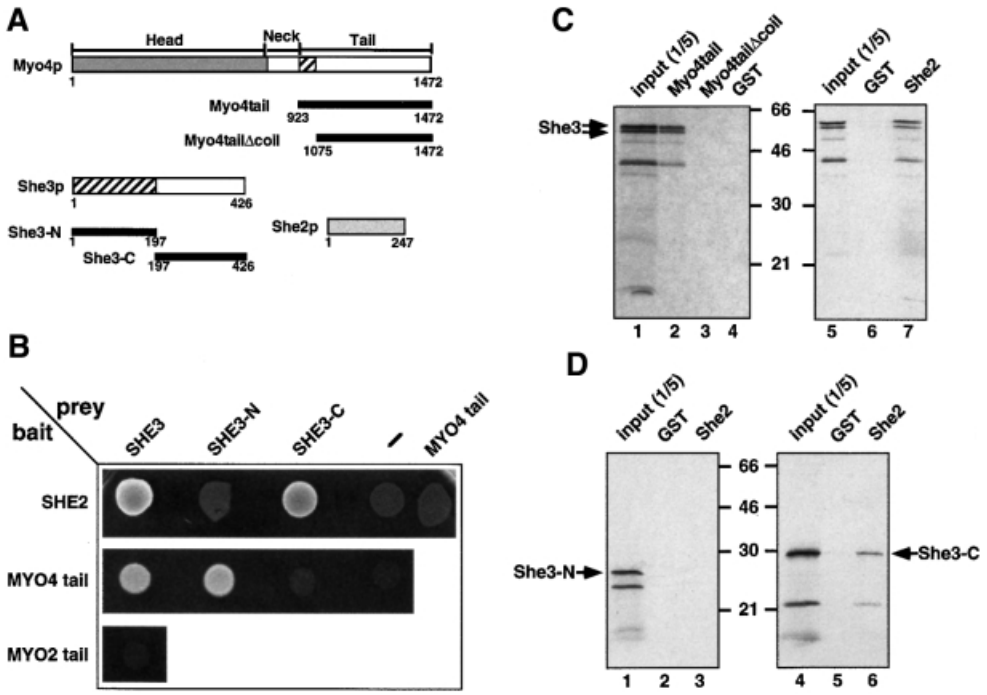

Fig. 1. She3p binds to the motor Myo4p and to She2p via different domains. (**A**) Schematic representation of the constructs used in the *in vivo* and *in vitro* interaction assays. Numbers below boxes correspond to amino acid position. Hatched boxes in Myo4p and She3p represent predicted coiled-coil regions. (**B**) Two hybrid interaction analysis. She2-, Myo4 tail- and Myo2 tail-Gal4 DNA binding domain fusions ('bait') were coexpressed with Gal4 activation domain alone or fusions ('prey') to Myo4p tail, She3p, She3p N-terminus and She3p C-terminus. Interaction was indicated by growth on medium lacking histidine. Whereas She2p showed interaction with full-length She3p and the She3p C-terminus, Myo4p tail interacted with She3p and She3p N-terminus. (**C**) *In vitro* interaction of She3p with Myo4p tail and She2p. Recombinant GST fusions of She2p, Myo4p tail, a Myo4 tail lacking the predicted coiled-coil domain or GST alone were immobilized to glutathione–Sepharose beads and incubated with *in vitro* translated ^{35}S-labelled She3p (double arrows). Bound She3p was eluted, and applied to an SDS–PAGE gel together with one-fifth of the *in vitro* translated She3p used for pulldown ('input'). Numbers indicate positions of molecular weight markers (in kDa). The band seen at 40 kDa is a degradation product of She3p. (**D**) *In vitro* interaction of She2p with the C-terminus of She3p. *In vitro* translated domains of She3p were affinity purified with GST–She2p beads as described above. Only the She3p C-terminal domain bound to GST–She2p.

ASH1 mRNA reinforces recruitment of She2p–*ASH1* RNA to the She3p–Myo4p complex.

Results

She3p can bind to both Myo4p and She2p

Previous work has shown that the She3 protein has an essential role in *ASH1* mRNA localization and colocalizes with both *ASH1* mRNA and the motor protein Myo4p in particles (Bertrand *et al*., 1998; Takizawa and Vale, 2000). Colocalization with Myo4p is independent of *ASH1* mRNA since it is also seen at stages where the RNA is not present (Jansen *et al*., 1996), suggesting a direct interaction of She3p with Myo4p. In order to test this and to identify the region of She3p that is responsible for its interaction with Myo4p, we followed two approaches. In a two-hybrid interaction assay we tested various parts of She3p for their binding to the C-terminal tail region of Myo4p (amino acids 923–1472, see Figure 1A). Both full-length She3p and the N-terminal half of She3p (amino acids 1–197) bind to the Myo4p tail in this assay whereas the C-terminal half of She3p (amino acids 197–426) cannot (Figure 1B). This interaction is specific since the tail of the related Myo2p myosin (amino acids 929–1574) does not bind to She3p (Figure 1B). Both the N-terminal region of She3p and the first 150 amino acids of the Myo4p tail have been predicted to form a coiled-coil structure that could serve as interaction domain (Haarer *et al*., 1994; Jansen *et al*., 1996).

In parallel studies, we wanted to elucidate the role of She2p in *ASH1* mRNA localization. In an attempt to identify interaction partners of She2p by a two-hybrid interaction approach we identified She3p as a putative binding partner (see Materials and methods). Out of 119 She2p-interacting clones isolated in an unbiased two-hybrid screen, 33 contained inserts spanning different portions of the *SHE3* open reading frame (ORF). The smallest overlapping fragment of all inserts covered the She3p C-terminus (amino acids 213–426), which lacks the coiled-coil part of She3p (data not shown). This prompted us to test directly for an interaction of She2p with different parts of She3p and with the Myo4p tail. Both full-length She3p and its C-terminal half showed an interaction with She2p (Figure 1B). In contrast, no binding was detected with either the She3p N-terminus or the Myo4p tail. In order to confirm our data, the *SHE2* and *SHE3* ORFs were swapped between the *GAL4* DNA-binding and activation domain vectors, which resulted in an identical activation pattern of the two-hybrid reporter genes (data not shown).

In order to verify the binding of She3p to She2p and Myo4p we tested whether the proteins associate *in vitro*. Recombinantly expressed glutathione *S*-transferase (GST) fused to She2p or Myo4p tail containing or lacking the coiled-coil region of Myo4 (GST–Myo4tail or

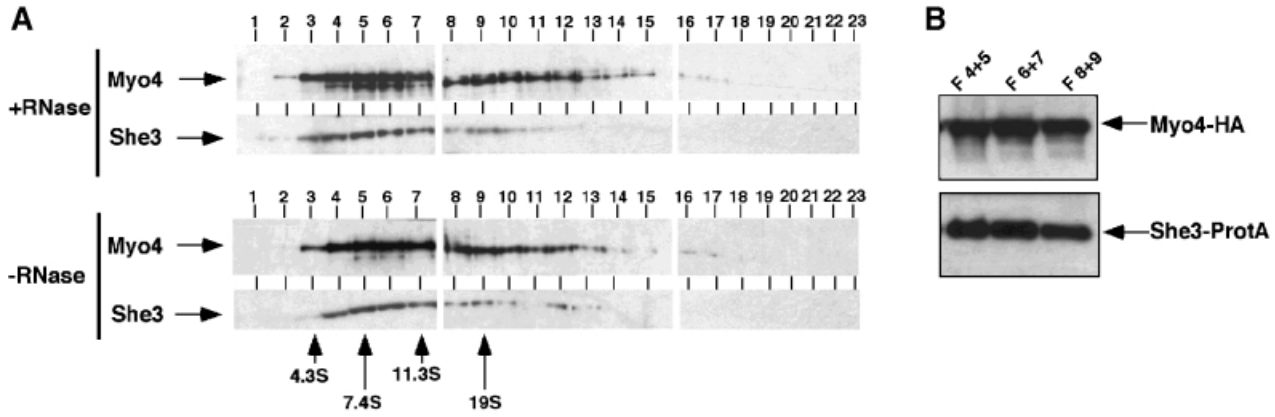

Fig. 2. She3p association with Myo4p *in vivo* is RNA independent. (**A**) Western blot analysis of a 5–25% sucrose gradient fractionation of a cell extract from strain RJY758 (*MYO4–HA6*, *SHE3-TEVProtA*, YEplac181-*ASH1*) after treatment with RNase A (upper panels) or mock treatment (lower panels). Numbers on top of the panels indicate fraction number (1 = top), numbers on the bottom indicate migration behaviour (in Svedberg units) of protein standards in a parallel gradient. (**B**) Immunoprecipitation of She3–ProtA by IgG–agarose beads from peak fractions of the RNase A-treated extracts reveals coprecipitation of Myo4p. Upper panel: western blot analysis using anti-HA antibody 12CA5; lower panel: western blot analysis using peroxidase–anti-peroxidase complex to detect She3–protein A fusion.

GST–Myo4tailΔcoil, respectively) was immobilized on glutathione–Sepharose beads. Full-length She3p and its N- and C-terminal domains were produced by *in vitro* translation in the presence of [^{35}S]methionine. GST–She2 as well as GST–Myo4tail beads but not beads with GST–Myo4tailΔcoil or GST alone precipitated *in vitro* translated She3p (Figure 1C). This demonstrates a direct interaction of the proteins. The C-terminal but not the N-terminal domain of She3p bound to GST–She2, supporting our two-hybrid assay results (Figure 1D). In contrast, unlike in the two-hybrid assay, the Myo4p tail domain did not bind significantly to either the N- or the C-terminal domain of She3p *in vitro* (data not shown).

To analyse the interaction of She3p and Myo4p *in vivo*, we generated a yeast strain that carries epitope-tagged versions of Myo4p fused to the haemagglutinin (HA) tag and She3p fused to two IgG-binding domains of protein A (Grandi *et al*., 1993). Cell extracts from this strain were fractionated on a 5–25% sucrose gradient. Both Myo4p–HA and She3p–ProtA comigrate on this gradient between 7.4S and 19S (Figure 2A). The comigration was independent of RNA since extensive RNase A digestion of the extract before fractionation resulted in a similar distribution of Myo4p–HA and She3p–ProtA in the gradient. RT–PCR analysis showed that no *ASH1* or *SIC1* RNA could be detected after RNase A treatment, indicating a successful removal of RNA (data not shown). In order to ensure that the comigration reflected an association of the two proteins, we immunoprecipitated She3p–ProtA. Precipitation of She3p–ProtA from the peak fractions (4–9) of the RNase A-treated extract resulted in coprecipitation of Myo4–HA (Figure 2B), indicating the tight RNA-independent association of these two proteins *in vivo*.

In summary, our results suggest that discrete domains of She3p bind to Myo4p and She2p, and implicate a role of She3p in linking the myosin tail to She2p.

She2p associates with ASH1 mRNA independently of She3p and Myo4p

Both Myo4p and She3p have been shown to associate with *ASH1* mRNA *in vivo* (Münchow *et al*., 1999; Takizawa and Vale, 2000). Disruption of *SHE2* abolishes Myo4p's association with the mRNA. We wondered whether the same is true for association of She3p and *ASH1* mRNA. Yeast strains were created that contain myc epitope-tagged versions of She3p either in the background of functional or non-functional She2p or Myo4p. Extracts were prepared from these strains and myc-tagged She3p precipitated using monoclonal anti-myc antibodies. Coprecipitated *ASH1* mRNA was detected by RT–PCR (Münchow *et al*., 1999).

Disruption of *SHE2* or *MYO4* did not significantly change the level of *ASH1* mRNA in the cell extract ('Total', Figure 3A, lanes 1–7). However, whereas *ASH1* mRNA could be detected in She3p–myc precipitates from both *MYO4*$^+$ and *myo4Δ* cell extracts ('Pellet', Figure 3A, lanes 5 and 7), She3p–myc did not coprecipitate *ASH1* mRNA in the absence of *SHE2* (Figure 3A, lane 6), suggesting an essential function of She2p for the association of both She3p and Myo4p (Münchow *et al*., 1999) with *ASH1* mRNA. This prompted us to check for an association of She2p with *ASH1* mRNA. Like She3p–myc, a myc epitope-tagged version of She2p coprecipitates *ASH1* mRNA (Pellet, Figure 3A, lane 2). In contrast to She3p, She2p still coprecipitates *ASH1* in the absence of Myo4p or She3p (Pellet, Figure 3A, lanes 3 and 4), indicating a *MYO4/SHE3*-independent association of She2p and *ASH1* mRNA *in vivo*.

To demonstrate the specificity of coprecipitation we used a myc-tagged version of Cse1p, a protein involved in nuclear export (Solsbacher *et al*., 1998). In addition, we tested for coprecipitation of the myc-tagged proteins with a second mRNA, *SIC1*, which shows a similar expression profile and abundance to *ASH1* (Schwob *et al*., 1994). Both controls demonstrate that *ASH1* mRNA specifically coprecipitates with She3p–myc and She2p–myc since no *ASH1* mRNA could be detected in Cse1p–myc precipitates and no significant amounts of *SIC1* mRNA were detected in the She protein immunopellets.

She2p binds directly to ASH1 mRNA

Since She2p associates with *ASH1* mRNA *in vivo* independently of She3p and Myo4p, we wondered if She2p might bind directly to *ASH1* mRNA and might therefore

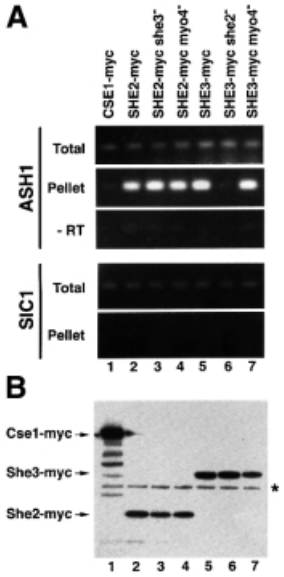

Fig. 3. Specific coprecipitation of *ASH1* mRNA with myc-tagged She3p and She2p. Myc-tagged proteins from cell extracts of strains containing or lacking functional *SHE* genes were precipiated with anti-myc antibody 9E11 coupled to magnetic beads essentially as described in Münchow *et al.* (1999). Eluted material was prepared for RT–PCR or western blot analysis. (**A**) RT–PCR analysis. A 247 bp fragment covering part of the *ASH1* 3′UTR or a 316 bp fragment covering the 3′ part of *SIC1* mRNA were amplified from total extract and immunoprecipitates of myc-tagged proteins. No PCR product was observed when reverse transcriptase was omitted ('–RT'). (**B**) To show equal efficiency of immunoprecipitations in myc-tagged strains, identical aliquots of the immunoprecipitates were separated on 10% SDS–PAGE and myc-tagged proteins detected by western blotting using anti-myc antibody 9E10. Lane 1, Cse1p–myc; lanes 2–4, She2p–myc; lanes 5–7, She3–myc. An asterisk marks the position of the antibody heavy chain.

be the *ASH1* RNA-binding protein. To test this, we used a GST pulldown assay (Trifillis *et al*., 1999). A recombinantly produced GST–She2 fusion protein was immobilized on glutathione–Sepharose beads. In parallel, GST alone was purified and similarly immobilized. ^{32}P-labelled *ASH1* mRNA and control transcripts were generated *in vitro* by SP6 polymerase. Transcripts were mixed with identical amounts of immobilized GST and GST–She2 proteins in the presence of competitor tRNA and the resulting protein–RNA complexes were purified (see Materials and methods). Bound RNA was eluted and aliquots were removed for quantification or applied to denaturing agarose or polyacrylamide gels. The results of the pulldown experiments are summarized in Figure 4A. No RNA was coprecipitated with GST alone (Figure 4B and data not shown). Similar negative results were obtained when we used a fusion of GST and the RNA-binding coat protein (Peabody, 1990) from phage MS2 (data not shown).

GST–She2p was able to bind specifically to full-length *ASH1* mRNA including the 5′ and 3′UTRs (Figure 4A). Furthermore, binding was also detected to shorter transcripts that contained at least one of the described RNA localization elements E1–E3 (Chartrand *et al*., 1999). Strongest binding (>50% of the input material precipitated) was observed to transcripts containing elements E1, E1 plus E2A/B ('ΔE3'), or E3 plus the remaining 3′UTR ('ΔE1ΔE2'). Each of these fragments has been shown to be able to localize a *lacZ* reporter RNA to the daughter cell (Chartrand *et al*., 1999). The shortest RNA fragment that bound to GST–She2p was a subfragment of the E3 localization element, element ASH1-U (also named U), which can also localize a reporter RNA (Gonzalez *et al*., 1999) (see also Figure 4C). In contrast, a mutant version of element U ('U*') with a disruption of the distal double-stranded stem abolished binding to She2p (Figure 4B, lane 9, and C). The disruption of this double-stranded RNA stem resulted in a loss of RNA localization *in vivo* (Gonzalez *et al*., 1999). No binding of GST–She2p was observed to RNAs lacking E elements ('ΔE elements', 'inter'), *ASH1* antisense RNA or RNA encoding yeast Srp54 protein (Hann and Walter, 1991) (Figure 4A and B).

Interestingly, a GST–She3p fusion protein was able to bind weakly to labelled *ASH1* RNA (data not shown). Approximately 15% of the input RNA coprecipitated with GST–She3p. However, in contrast to GST–She2p, binding was not specific since no significantly stronger precipitation of *ASH1* full-length RNA than of control RNAs (antisense *ASH1* or *SRP54* RNA) was observed in our assay (data not shown).

To demonstrate that the interaction of GST–She2p with *ASH1* mRNA is authentic we used a second method to test for protein–RNA binding. Labelled RNAs covering localization elements ASH1-U, or -U* (76 nucleotides each) were mixed with increasing amounts of purified GST or GST fused to She2p or She3p and complex formation was determined by a mobility shift assay (Figure 5A). GST, GST–She3p or GST–MS2 (data not shown) failed to bind to ASH1-U whereas GST–She2p formed a complex with element ASH1-U (black arrowhead). Similar binding was observed to E3 (Supplementary data, available at *The EMBO Journal* Online) as well as a weak but significant binding to the E2B element (data not shown). In contrast, no mobility shift was observed when She2p was incubated with mutant U* (Figure 5A) or another double-stranded RNA, iron-response element (IRE, Figure 5C), indicating that She2p does not recognize all stem–loop-forming RNA structures.

The mobility shift assay also allowed us to address the question of binding cooperativity between She2p, She3p and ASH1-U. The presence of GST–She3p but not of GST in a binding reaction of GST–She2p and ASH1-U enhanced the complex formation of She2p and *ASH1* RNA (Figure 5B). In addition, a new complex with lower mobility (open arrow) appeared, suggesting the formation of a higher order complex.

In summary, our analysis demonstrates the direct binding of *ASH1* mRNA to She2p *in vivo* and *in vitro*. Binding of She2p to the mRNA depends on the presence of functional localization elements E1–E3 within the RNA and is enhanced by She3p.

She2p moves to the bud in an ASH1 RNA-dependent manner

The association of She2p and *ASH1* mRNA was surprising because of previous findings that, unlike She3p and Myo4p, She2p does not colocalize with *ASH1* (Jansen *et al*., 1996; Bertrand *et al*., 1998). We wondered whether the apparent lack of colocalization could be due to an

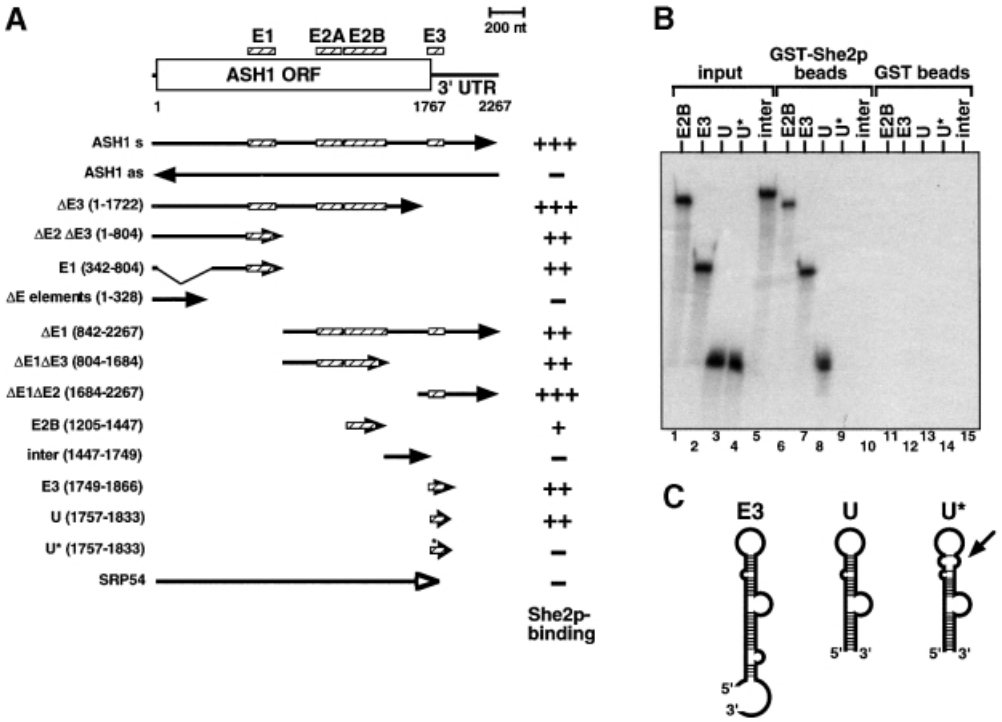

Fig. 4. Purified GST–She2p binds *ASH1* RNA *in vitro* through the localization elements E1–E3. (**A**) Overview of the results of *ASH1*–GST–She2p pulldown experiments. At the top of the panel *ASH1* mRNA is sketched with the positions of the localization elements E1, E2A, E2B and E3 (hatched bars). Numbers below indicate nucleotide position (AUG = 1). Arrows indicate the start and end of the RNAs used in the pulldown experiments. Numbers in parentheses on the left indicate the start and end of the RNAs on the nucleotide level. The right column indicates relative recovery of input RNA on the glutathione beads. +++, recovery >50%; ++, >35%; +, >15%; –, <10%. Results are mean values of three to five independent experiments. (**B**) Representative denaturing polyacrylamide gel showing specific precipitation of ^{32}P-labelled localization elements E2B, E3 and ASH1-U by GST–She2p (lanes 6–8) but not of the mutant U* or an RNA lacking localization elements ('inter', lanes 9 and 10). No binding of RNA was observed when beads where loaded with GST (lanes 11–15). Lanes 1–5 show input RNAs. (**C**) Schematic overview of predicted secondary structures of localization elements E3, ASH1-U and U*. The arrow indicates disrupted doubled-stranded RNA stem in mutant element U*.

inaccessibility of She2p by anti-She2p antibodies once the protein has become part of the putative localization particle. We therefore used a 9-fold myc epitope to tag She2p at the C-terminus with the rationale that a sufficient number of myc epitopes would stick out of the localization particle to detect the tagged protein by indirect immunofluorescence.

Yeast strains were constructed that express a functional myc9-tagged She2p and carry either a high-copy plasmid with *ASH1* under the control of its own promoter (2μ *ASH1*) or of the inducible GAL1 promoter (GAL1-*ASH1*). Although *ASH1* mRNA is normally only expressed and transported in late anaphase cells, it has the potential to localize to the bud at earlier stages of the cell cycle when expressed from a heterologous promotor (Long *et al.*, 1997).

In a population of cells that have a higher dosage of *ASH1* (2μ-ASH1), ~40% (18/47 counted) of anaphase cells with an *ASH1* signal at the bud tip also show a She2p–myc9 signal overlapping with the RNA staining (Figure 6A and B). In cells carrying the GAL1-*ASH1* plasmid, She2p–myc is detected throughout the cytoplasm under non-inducing conditions (Figure 6D). Some staining is also visible at the position of the nucleus (Figure 6, compare D with DAPI staining in F), indicating that She2p might be distributed between both nucleus and cytoplasm. Upon induction of *ASH1* by addition of galactose to the culture, the cells show an additional strong staining of She2p–myc at the bud tip (Figure 6G). This staining overlaps with the position of *ASH1* mRNA as detected by *in situ* hybridization (Figure 6H). No She2p–myc staining at the bud tip was detected when cells carrying a control plasmid without the *ASH1* gene were induced (Figure 6K). In addition, no accumulation of She2p–myc at the bud tip was observed when *ASH1* was induced in a strain carrying a deletion of *SHE3* (data not shown). In contrast to She2p, She3p–myc localizes to the bud tip independently of *ASH1* induction (Figure 6N).

Our results demonstrate that She2p moves to the bud tip upon *ASH1* expression and suggest She2p is transported to its destination site together with *ASH1* mRNA. The data are supported by recent findings of Takizawa and Vale (2000) that an epitope-tagged version of She2p with 13 myc epitopes colocalizes with an *ASH1* RNA-containing particle.

She2p binds to Myo4p–She3p in an ASH1-dependent manner

How is She2p recruited to the daughter cell tip? Both Myo4p and She3p can localize to the daughter cell tip independently of *ASH1* RNA. Does She2p therefore bind in an *ASH1*-dependent manner to Myo4p–She3p to become localized? To test this idea, we generated strains containing She proteins with different epitopes (Myo4p–HA6, She3p–ProtA, She2p–myc3) and a plasmid that allowed galactose-dependent *ASH1* RNA induction ('+ASH1') or the induction of an unrelated RNA ('–ASH1'). Cell extracts were prepared after galactose

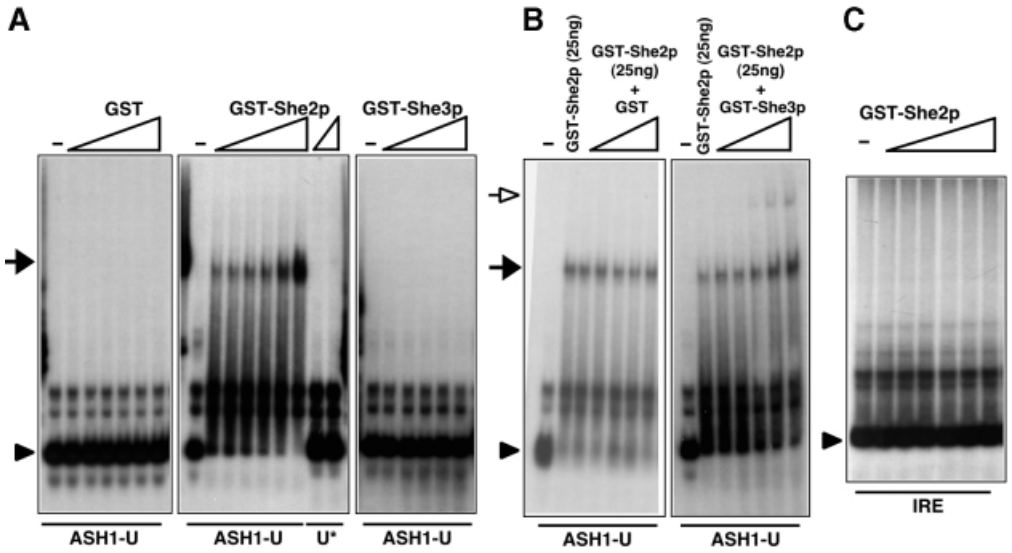

Fig. 5. She2p binding to ASH1-U is specific and enhanced by She3p. Probes used are indicated at the bottom of each panel, proteins at the top. (**A**) RNA mobility shift assay using ^{32}P-labelled probes of ASH1-U or mutant U* and increasing concentrations of GST, GST–She2p (2.5, 5.0, 7.5, 10, 20, 40 ng/µl) or GST–She3p (10, 20, 30, 40, 60 ng/µl). The arrowhead indicates the position of free probe and the black arrow the position of an ASH1-U RNA complex with GST–She2p that cannot be detected with GST–She3p or mutant U*. (**B**) Mobility shift using constant GST–She2p (2.5 ng/µl) and increasing concentrations of GST or GST–She3p (10, 20, 30, 40, 60 ng/µl). Increasing the amount of She3p but not of GST enhances She2p–ASH1-U complex formation (black arrow) and leads to the formation of an RNA–protein complex with lower mobility (open arrow). (**C**) Mobility shift assay using the IRE as probe. No complex formation is observed.

induction, and She3p–ProtA precipitated with IgG–agarose beads. Coprecipitated proteins were detected by western blotting using antibodies against the HA or myc epitope (Figure 7). Whereas coprecipitation of Myo4p with She3p was independent of *ASH1* induction (Figure 7, lanes 4–6), She2p was enriched in immune pellets from extracts of cells where *ASH1* had been induced (Figure 7, compare lanes 5 and 6). To prove inevitably that the band detected at the position of She2–myc is not a breakdown product of She3–ProtA, we used a control strain that expresses Myo4–HA and She3p–ProtA but lacks a myc epitope ('control', Figure 7, lanes 1 and 4). The absence of a band at the size of She2p–myc clearly shows that the detected band in lane 6 corresponds to She2–myc. Interestingly, we also observed a very weak She2p band in precipitates from cells without overexpressed *ASH1* (Figure 7, lane 5). This could reflect a weak RNA-independent She2p–She3p binding or might be due to low amounts of endogenous *ASH1* mRNA in the non-induced cells.

We conclude from our data that, *in vivo*, *ASH1* RNA reinforces the association of She2p with the Myo4p–She3p complex.

Discussion

The interaction network of Myo4p, She2p, She3p and *ASH1* mRNA that we identified provides a first detailed description of how a localized mRNA is tethered to its cognate motor protein.

Tethering of localized RNA and motor protein depends on the function of two She proteins whose role in RNA localization has previously not been understood. *ASH1* mRNA is bound by an RNA-binding zipcode-specific protein, She2p. A motor protein-associated linker protein, She3p, interacts with this RNA-binding protein. She3p appears to bind the motor, Myo4p, and the RNA-binding protein, She2p, via different domains.

Several experimental findings demonstrate that She2p is the crucial RNA-binding protein. *In vivo*, deletion of *MYO4* or *SHE3* does not alter She2p's ability to coprecipitate *ASH1* mRNA, suggesting a direct and motor protein-independent association of She2p with the RNA. She2p can bind *ASH1* mRNA directly *in vitro* and this binding occurs via the defined *ASH1* RNA localization elements E1, E2A/B and E3. Deletion analysis showed that transcripts with only one localization element coprecipitated with GST–She2p as efficiently as full-length RNA. This suggests that She2p can bind independently to any of the localization elements and does not have a preference for a specific element. Similar results have been obtained by an *in vitro* cross-linking approach using recombinant She2p and RNA localization elements (R.Long, personal communication).

How can She2p recognize all three independent *ASH1* RNA localization zipcodes? The differences in sequence of the three localization elements strongly suggest a common structural feature. E1, E3 and ASH1-U have been predicted to form double-stranded stem–loop structures with several bulges (Chartrand *et al*., 1999; Gonzalez *et al*., 1999). Structure prediction of the E2B localization element also suggests the presence of a stable stem–loop structure (data not shown). Mutations within the terminal stem of E1 and E3 disrupt the localizing activity of the zipcode elements (Chartrand *et al*., 1999). Consistent with these data we have shown that She2p binds directly to the shortest wild-type zipcode (ASH1-U) but not to a mutant version with a partially disrupted stem (Gonzalez *et al*., 1999), suggesting that She2p might recognize the terminal stem–loop structure of the zipcodes.

She2p does not show any sequence homology to other proteins in the databases. In addition, She2p does not

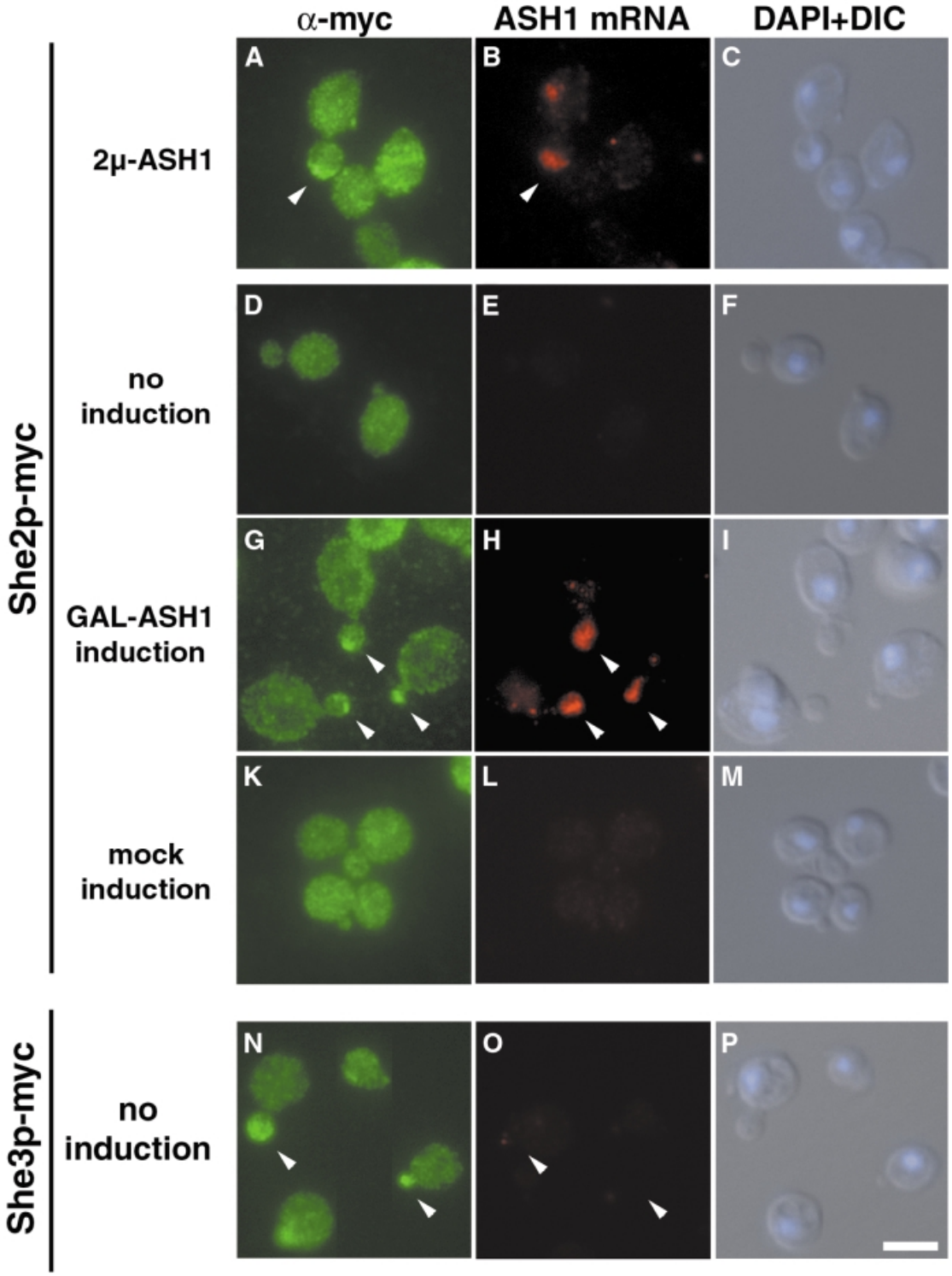

Fig. 6. She2p–myc9 localizes to the bud tip upon *ASH1* expression. Overexpression of *ASH1* mRNA from a high-copy plasmid (A–C) or from the heterologous *GAL1* promoter (G–H) induces a shift of She2p localization to the bud tip (arrowheads). Localization of She3–myc6 to the bud tip is independent of *ASH1* expression (N–P). A combination of indirect immunofluorescence against myc-tagged proteins and *in situ* hybridization against *ASH1* mRNA was performed as described in Materials and methods. Immunofluorescence staining against She2p–myc9 is shown in (**A**), (**D**), (**G**) and (**K**), whereas staining in (**N**) reflects She3p–myc6 localization. (**B**), (**E**), (**H**), (**L**) and (**O**) show localization of *ASH1* mRNA by *in situ* hybridization using CY3-labelled *ASH1* antisense oligos. (**C**), (**F**), (**I**), (**M**) and (**P**) are composite images of differential interference contrast (DIC) and DNA staining by DAPI. Bar, 5 μm.

contain sequence motifs found in other classes of RNA-binding proteins (Query *et al*., 1989; Bycroft *et al*., 1995; Adinolfi *et al*., 1999). We propose that She2p represents a novel type of RNA-binding protein.

What is the function of the other She protein essential for *ASH1* mRNA localization, She3p? The similar localization pattern of She3p and Myo4p at all stages of the cell cycle suggested a tight association of She3p and Myo4p

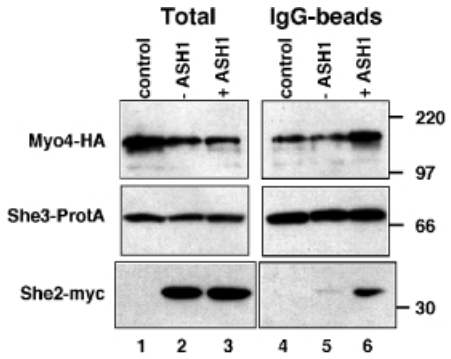

Fig. 7. Coprecipitation of She2–myc with She3–ProtA and Myo4–*HA* upon *ASH1* RNA overexpression. Western blot analysis of cell extracts from strains RJY750 (SHE3–ProtA, MYO4–HA6, 'control'), RJY756 (SHE3–ProtA, MYO4–HA6, SHE2–myc3, pGAL1; '–ASH1') and RJY757 (SHE3–ProtA, MOY4–HA6, SHE2–myc3, pGAL1-*ASH1*; '+ASH1'), and corresponding pellets from an anti-protein A precipitation ('IgG-beads'). The blot was cut into three pieces and probed with antibodies against HA, myc or protein A. Numbers on the right indicate the positions of size markers (in kDa).

(Jansen *et al*., 1996). Our results indicate that this association is direct. First, Myo4p and She3p copurify in a two-step purification in the absence of RNA. Secondly, She3p binds to the Myo4p C-terminal domain but not to that of the related Myo2p myosin in a two-hybrid interaction trap. Interaction requires the presence of She3p's predicted coiled-coil domain (Jansen *et al*., 1996). Thirdly, a GST fusion of the C-terminal myosin tail binds directly to an *in vitro* translated She3p. This binding depends on the presence of coiled-coil domains within the Myo4p tail (amino acids 923–1075). Taken together, two-hybrid and GST pulldown data suggest an interaction of Myo4 tail and She3p through their coiled-coil domains. However, so far we have not been able to demonstrate this interaction *in vitro*. Coiled-coil domains within class V myosin tails have been suggested to be essential only for heavy chain dimerization (Mermall *et al*., 1998). Our findings might add an additional function to this domain of class V myosins.

In summary, our data demonstrate a direct interaction of She3p and the myosin motor protein Myo4p. Similar findings have recently been published by Takizawa and Vale (2000).

Whereas She3p's N-terminal half seems to bind to the myosin motor, its C-terminus is involved in She2p binding. A direct *ASH1* RNA-independent binding of She2p and She3p is suggested by our *in vitro* pulldown experiments. In contrast, our *in vivo* experiments indicate that *ASH1* mRNA reinforces the She2p–She3p interaction. Overexpression of *ASH1* from a strong *GAL1* promoter strongly increases the quantity of She2p coprecipitating with She3p and Myo4p. Consistent with this finding, She2p localization changes upon *ASH1* expression and, like *ASH1* mRNA, She2p becomes concentrated at the bud tip. In addition to *ASH1*, this movement depended on the presence of She3p (data not shown). Our finding that She3p enhances She2p–*ASH1* mRNA complex formation suggests some cooperativity of binding between She2p, She3p and *ASH1* mRNA that might result in a more stable RNA–protein complex.

Our results suggest a model in which *ASH1* mRNA is associating with the RNA-transporting motor protein Myo4p through the interaction with two She proteins, She2p and She3p. She2p seems to be the RNA-binding protein of the RNA–motor protein complex. She3p's major role seems to be to form a bridge between the heavy chain of the myosin motor, Myo4p, and the She2p–*ASH1* RNP, and it can therefore be considered as a specific adapter for the *ASH1* RNP.

It is interesting to note that, although currently no She3p homologue has been identified, the protein shows functional analogy to the *Drosophila* swallow (Swa) protein involved in bicoid RNA localization (Schnorrer *et al*., 2000). Like Swa, She3p binds directly to a motor protein (cytoplasmic dynein or myosin, respectively) via its coiled-coil domain. Furthermore, localization of She3p and Swa to their destination sites is independent of their cognate RNA. Swa contains a putative RNA-binding motif and might therefore bind the transported RNA directly, although this has not been shown.

Although our data suggest that Myo4, She2p and She3p are part of the *ASH1* mRNP that is localized to the daughter cell tip, we have no evidence that they are the only proteins of this complex. A full description of the protein content of the *ASH1* mRNP must await its biochemical purification.

Materials and methods

Yeast strains and methods

All yeast strains used in this study are listed in Table I and were derived from W303a (Rothstein, 1983) with the exception of RJY786–RJY791, which have an RS453 background (Segref *et al*., 1997). Sequences of applied oligonucleotides are published in Supplementary Table II. Media preparation and manipulation of yeast cells were carried out essentially as described (Adams *et al*., 1997). Transformation was performed according to Gietz and Schiestl (1995). Gene disruption of various *SHE* genes with the *Schizosaccharomyces pombe HIS3* marker gene was achieved using a PCR-based method described by Wach *et al*. (1997). In all cases of PCR applications, proofreading polymerases were used. Amplified constructs were verified by sequencing.

Epitope tagging of MYO4, SHE2 and SHE3

Epitope tagging of *SHE2* with three myc epitopes and of *MYO4* with six HA epitopes has been described (Jansen *et al*., 1996). In order to generate versions of *SHE2* with nine myc epitopes and of *SHE3* with two ZZ domains of protein A we followed the 'one-step tagging' method described by Knop *et al*. (1999). Transformants were checked by Southern analysis for correct integration. All epitope-tagged proteins were fully functional.

Two-hybrid interaction analysis

Myosin tail-encoding regions of the *MYO2* ORF (amino acids 929–1574) and *MYO4* ORF (amino acids 923–1472) were amplified using primer pairs omyo2-BH1 and omyo2-*Pst*I or omyo4-2hyb2 and omyo4-2hyb3. The *Bam*HI and *Pst*I sites, or the *Eco*RI and *Bam*HI sites, respectively, generated this way were used to clone the PCR products into the bait vector pBTM116. The *SHE3* ORF was amplified using primers RJO20 and RJO21, creating *Eco*RI or *Bam*HI sites at the ends. *SHE3-N* (encoding amino acids 1–197) and *SHE3-C* (encoding amino acids 197–426) were amplified similarly, using primer pairs RJO20 and RJO89 or RJO21 and RJO90, respectively. Amplified and digested DNA fragments were cloned into pGAD424 (Clontech Laboratories). The *SHE2* coding region was amplified using primers RJO18 and RJO19, digested with *Eco*RI and *Bam*HI and cloned into the bait vector pGBDU-C1 (James *et al*., 1996). Yeast strain L40 (Nonaka *et al*., 1995) or PJ694A (James *et al*., 1996) was co-transformed with the resulting bait plasmids and pGAD424-*SHE3* constructs. Transformants were selected on appropriate medium and subsequently tested for activation of the *lexA-HIS3* (L40) or *GAL1-HIS3* (PJ694A) reporter genes.

Table I. Yeast strains used in this study

Name	Relevant genotype	Source
L40	*Mat***a**, *hisD200, trp1-901, leu2-3,112, ade2, LYS2::*(4lexAop-*HIS3), URA3::*(8lexAop-*lacZ), GAL4*	Nonaka *et al*. (1995)
PJ69-4α	*Matα*, *trp1-901, leu2-3,112, ura3-52, his3-200, gal4Δ*; *gal80Δ*; *GAL2-ADE2, LYS2::GAL1-HIS3, met2::GAL7-lacZ*	James *et al*. (1996)
RJY375	*Mat***a**, *pep4::URA3, CSE1–myc9::HIS3,* YEplac181-*ASH1*	Münchow *et al*. (1999)
RJY505	*Matα*, *HO-ADE2, pep4::LEU2, SHE3–myc6,* YEplac195-*ASH1*	D.Djandji, unpublished
RJY574	*Matα*, *HO-ADE2, pep4::LEU2, SHE3–myc6, myo4::HIS3MX6,* YEplac195-*ASH1*	this work
RJY634	*Mat***a**, *pep4::URA3, SHE3–myc6, MYO4–HA6, she2::HIS3MX6,* YEplac181-*ASH1*	this work
RJY635	*Mat***a**, *SHE2myc3::HIS3MX6,* YEplac181-*ASH1*	this work
RJY636	*Mat***a**, *SHE2myc3::HIS3MX6, she3::URA3,* YEplac181-*ASH1*	this work
RJY750	*Matα*, *HO-ADE2, pep4::URA3, SHE3-TEVProA::HIS3MX6, MYO4–HA6*	this work
RJY756	*Mat***a**, *HO-ADE2, pep4::URA3, SHE3-TEVProA::HIS3MX6, MYO4–HA6, SHE2–myc3,* p415-*GAL1*	this work
RJY757	*Mat***a**, *HO-ADE2, pep4::URA3, SHE3-TEVProA::HIS3MX6, MYO4–HA6, SHE2–myc3,* p415-*GAL1-ASH1*	this work
RJY758	*Matα*, *HO-ADE2, pep4::URA3, SHE3-TEVProA::HIS3MX6, MYO4–HA6,* YEplac181-*ASH1*	this work
RJY785	*Mat***a**, *SHE2–myc3::HIS3MX6, myo4::URA3,* YEplac181-*ASH1*	this work
RJY786	*Mat***a**, *mex67::HIS3, SHE2myc9::klTRP1,* pUN100-*MEX67,* YEplac195	this work
RJY787	*Mat***a**, *mex67::HIS3, SHE2myc9::klTRP1,* pUN100-*MEX67,* YEplac195-*ASH1*	this work
RJY788	*Mat***a**, *mex67::HIS3, SHE2myc9::klTRP1,* pUN100-*MEX67,* p416-*GAL1*	this work
RJY789	*Mat***a**, *mex67::HIS3, SHE2myc9::klTRP1,* pUN100-*MEX67,* p416-*GAL1-ASH1*	this work
RJY791	*Mat***a**, *mex67::HIS3, SHE3myc9::klTRP1,* pUN100-*mex67-5,* p416-*GAL1-ASH1*	this work

Strains RJY375–RJY785 are derivatives of W303a (also named K699) with the following full genotype: *Mat***a**, *ade2-1, trp1-1, can1-100, leu2-3,112, his3-11,15, ura3, GAL, psi*$^{+}$. Strains RJY786–RJY791 are derived from RS453, whose genotype is: *Mat***a**, *ade2, his3, leu2, trp1, ura3, his3*.

For the two-hybrid interaction screen with *SHE2*, PJ694A containing pGBDU-*SHE2* was transformed with three *GAL4* activation domain libraries carrying yeast genomic DNA fragments in different reading frames (James *et al*., 1996). Of ~9 × 10^6 transformants, 1362 were selected in the first round because they were able to grow on medium lacking histidine. Of these clones, 119 grew on his^{-}ade^{-} medium and were subjected to further analysis by plasmid rescue, PCR–restriction analysis of the inserts and sequencing. Thirty-three of the clones analysed contained either full-length *SHE3* or 3′ fragments of the *SHE3* ORF encoding the She3p C-terminus.

In situ hybridization and immunofluorescence

For *ASH1* induction, we used a centromeric plasmid containing *ASH1* under the control of the strong GAL1 promoter. A fragment of *ASH1* (from *ASH1* ATG to nucleotide 510 of the 3′UTR) was amplified using primers RJO141 and RJO142. After digestion with *Bam*HI and *Xho*I, the DNA fragment was cloned into p415-GAL1 or p416-GAL1 (Mumberg *et al*., 1994). The resulting plasmids and the empty vectors were transformed into yeast resulting in strains RJY788 (*SHE2–myc9*, p416-*GAL1*), RJY789 (*SHE2–myc9*, p416-*GAL1-ASH1*), RJY756 (*MYO4–HA6*, *SHE2–myc3*, *SHE3-TEVProtA*, p415-*GAL1*) and RJY757 (*MYO4–HA6, SHE2–myc3*, *SHE3-TEVProtA*, p415-*GAL1-ASH1*). For induction, stationary-phase cells grown overnight in 2% raffinose minimal medium lacking uracil were diluted into YEP/2% raffinose and grown for two generations at 30°C. Galactose was added to a final concentration of 3% and cells were induced for 1 h before fixation or cell lysis with glass beads. Combined *in situ* hybridization against *ASH1* mRNA and immunofluorescence against myc-tagged proteins were performed as described (Long *et al*., 1997) with the modification that anti-mouse Alexa-488 antibodies were used as secondary antibodies (diluted 1:1000) and that all manipulations were performed on multiwell slides in order to minimize antisense probe and antibody consumption.

Immunoprecipitation of epitope-tagged proteins

Immunoprecipitation of myc-tagged proteins and subsequent detection of *ASH1* or *SIC1* mRNAs by RT–PCR were performed essentially as described (Münchow *et al*., 1999). Two changes have been introduced to the protocol. The new breakage buffer A contained 50 mM HEPES–KOH pH 7.3, 20 mM potassium acetate, 2 mM EDTA, 0.1% Triton X-100, 5% glycerol and a protease inhibitor cocktail (Roche). The anti-mouse IgG2a magnetic beads (Dynal) were blocked three times for 10 min in breakage buffer containing tRNA (0.1 mg/ml). Three independent RT–PCRs were performed from each immune pellet in order to minimize RT–PCR-dependent amplification variation.

Immunoprecipitation of She3–ProtA and detection of coprecipitated proteins were performed as follows. Logarithmically growing cells (3 × 10^8) of strains RJY750, RJY756 and RJY757 (induced by addition of 3% galactose) were disrupted with glass beads in 300 µl of breakage buffer containing a protease inhibitor cocktail. Extracts were cleared by centrifugation (2 min at 5000 *g*). After addition of IgG–agarose beads (Sigma), extracts were incubated for 1 h at 4°C. Beads were pelleted and washed with breakage buffer containing 50 mM potassium acetate. Bound proteins were eluted with hot Laemmli buffer. Equivalent amounts of the cell extract (total) and the eluted proteins (pellet) were separated by PAGE and blotted, and epitope-tagged proteins were detected using monoclonal antibodies 12CA5 (anti-HA), 9E10 (anti-myc) or peroxidase–anti-peroxidase conjugate (PAP; Sigma).

Cell extract fractionation by sucrose gradient centrifugation

Logarithmically growing cells (2 × 10^9) of strain RJ758 (*SHE3-TEVProtA*, *MYO4–HA6*, YEplac181-*ASH1*) were pelleted and the pellet resuspended in an equal volume of 2× breakage buffer B (100 mM HEPES–KOH pH 7.3, 100 mM potassium acetate, 10 mM magnesium acetate, 0.2% Triton X-100, 10% sucrose) including protease inhibitors. After cell lysis with glass beads, extracts were clarified by centrifugation (10 min at 1000 *g*). Mg-ATP was added to a final concentration of 5 mM and extracts were treated at 4°C for 10 min either with 10 µg of RNase A or with 400 U of RNase inhibitor (Promega). Extracts were loaded onto a 5–25% sucrose gradient (in 1× breakage buffer B without Triton X-100) and centrifuged at 4°C for 16 h at 100 000 *g*. Fractions (500 µl) were collected from the top and aliquots separated on 8% PAGE. After blotting, the membrane was cut into two halves and probed for the presence of either She3p–ProtA or Myo4p–HA6.

GST pulldowns and electrophoretic mobility shift assays

For expression of recombinant MS2, She2p, She3p and Myo4p tail, we generated fusions to GST in pGEX4T2 (Pharmacia). The ORF of MS2 coat protein (Peabody, 1990) was amplified from pG14-MS2-GFP (Bertrand *et al*., 1998) using primers that added *Bam*HI and *Xho*I sites at the 5′ or 3′ terminus (RJO261 and RJO262). The *SHE2* ORF was cloned as a *Bam*HI–*Eco*RI fragment in-frame with GST. Restriction sites were generated by PCR with primers RJO232 and RJO233. Similarly, DNA fragments carrying the *SHE3* ORF or *MYO4* coding for amino acids 923–1471 (‘Myo4p tail’) or amino acids 1075–1471 (‘Myo4p tailΔcoil’) with new *Bam*HI and *Sal*I sites were created by PCR and cloned in-frame with GST. Expression and purification procedures of all fusion proteins are available as Supplementary data.

For *in vitro* translation of She3p, the *SHE3* ORF was amplified by PCR using oligonucleotides RJO230 and RJO231. *SHE3-N* and *SHE3-C* were generated using primer pairs RJO230 and RJO271 or RJO231 and RJO272. The PCR products were cloned as a *Bam*HI–*Eco*RI fragment into pGEM-3Z. Coupled *in vitro* transcription–translation in the presence of ^{35}S-labelled methionine was performed with the TNT Quick system (Promega) according to the manufacturer’s suggestions. An aliquot of the

translation extract (1/10) was incubated for 60 min at room temperature with immobilized GST fusion proteins in 1 ml of binding buffer (50 mM NaCl, 20 mM Tris–HCl pH 8.0, 0.5% NP-40, 0.1 mg/ml insulin) and washed four times with binding buffer lacking insulin. Bound proteins were eluted with hot Laemmli buffer, separated by 12% SDS–PAGE, and labelled proteins detected by autoradiography.

For pulldown experiments with *in vitro* transcribed RNAs and immobilized GST fusion proteins, we followed the protocol of Trifillis *et al*. (1999). Full-length SRP54 (a gift from M.Pool) and *ASH1* genes were cloned into pGEM-3Z and desired subfragments of *ASH1* were created by successive deletion of *ASH1* using convenient restriction sites. A detailed cloning strategy of the diverse fragments is published as Supplementary data. [^{32}P]CTP-labelled *in vitro* transcripts were generated using Promega's Riboprobe SP6 transcription system. Labelled RNA (10^6 c.p.m.) was added to 1 µg of immobilized GST fusion protein in 400 µl of RNA-binding buffer (RBB: 10 mM Tris–HCl pH 7.5, 150 mM KCl, 1.5 mM $MgCl_2$) containing 10 U of RNasin (Promega). After binding at 4°C for 1 h, beads were pelleted, washed with RBB containing 1 mg/ml heparin followed by four washes with RBB with 0.1% Triton X-100. RNA was extracted from the beads and resuspended in 50 µl of TE. One microlitre was used for quantitation using Cerenkov counting and 5 µl were loaded onto denaturing polyacrylamide or agarose gels.

For electrophoretic mobility shift analysis, we followed the protocol of Black *et al*. (1998). Increasing amounts of recombinant proteins were mixed with *in vitro* transcribed and labelled RNAs. Assembled complexes were separated from unbound probe by electrophoresis for 5 h at 170 V through a 5% polyacrylamide gel in 0.5× TBE.

Supplementary data

Supplementary data to this paper are available at *The EMBO Journal* Online.

Acknowledgements

We thank U.von Ahsen, P.Chartrand, E.Hurt, P.James, M.Pool, E.Schiebel and W.Zachariae for plasmids and strains, D.Görlich, F.Weismann and G.Merdes for help with recombinant protein expression, R.Long and R.Singer for communicating results prior to publication. We also thank M.Kiebler and A.Jaedicke for comments on the manuscript. R.-P.J. is a recipient of a grant from the DFG (JA696/2).

References

Adams,A., Gottschling,D.E., Kaiser,C.A. and Stearns,T. (1997) *Methods in Yeast Genetics*. Cold Spring Harbor Laboratory Press, Cold Spring Harbor, NY.

Adinolfi,S., Bagni,C., Castiglione Morelli,M.A., Fraternali,F., Musco,G. and Pastore,A. (1999) Novel RNA-binding motif: The KH module. *Biopolymers*, **51**, 153–164.

Bashirulla,A., Cooperstock,R.L. and Lipshitz,H.D. (1998) RNA localization in development. *Annu. Rev. Biochem.*, **67**, 335–394.

Bassell,G.J., Oleynikov,Y. and Singer,R.H. (1999) The travels of mRNAs through all cells large and small. *FASEB J.*, **13**, 447–454.

Bertrand,E., Chartrand,P., Schaefer,M., Shenoy,S.M., Singer,R.H. and Long,R.M. (1998) Localization of ASH1 mRNA particles in living yeast. *Mol. Cell*, **2**, 437–445.

Black,D.L., Chan,R., Min,H., Wang,J. and Bell,L. (1998) The electrophoretic mobility shift assay for RNA binding proteins. In Smith,C.W.J. (ed.), *RNA–Protein Interactions*. Oxford University Press, Oxford, UK, pp. 109–136.

Bobola,N., Jansen,R.-P., Shin,T.H. and Nasmyth,K. (1996) Asymmetric accumulation of Ash1p in postanaphase nuclei depends on a myosin and restricts yeast mating-type switching to mother cells. *Cell*, **84**, 699–709.

Bycroft,M., Grünert,S., Murzin,A.G., Proctor,M. and St Johnston,D. (1995) NMR solution structure of a dsRNA binding domain from *Drosophila* staufen protein reveals homology to the N-terminal domain of ribosomal protein S5. *EMBO J.*, **14**, 3563–3571.

Capri,M., Santoni,M.J., Thomas-Delaage,M. and Ait-Ahmed,O. (1997) Implication of a 5′ coding sequence in targeting maternal mRNA to the *Drosophila* oocyte. *Mech. Dev.*, **68**, 91–100.

Carson,J.H., Worboys,K., Ainger,K. and Barbarese,E. (1997) Translocation of myelin basic protein mRNA in oligodendrocytes requires microtubules and kinesin. *Cell Motil. Cytoskel.*, **38**, 318–328.

Chartrand,P., Meng,X.-H., Singer,R.H. and Long,R.M. (1999) Structural elements required for the localization of *ASH1* mRNA and of a green fluorescent protein reporter particle *in vivo*. *Curr. Biol.*, **9**, 333–336.

Cosma,M.P., Tanaka,T. and Nasmyth,K. (1999) Ordered recruitment of transcription and chromatin remodeling factors to a cell cycle- and developmentally regulated promoter. *Cell*, **97**, 299–311.

Evangelista,M., Blundell,K., Longtine,M.S., Chow,C.J., Adames,N., Pringle,J.R., Peter,M. and Boone,C. (1997) Bni1p, a yeast formin linking Cdc42p and the actin cytoskeleton during polarized morphogenesis. *Science*, **276**, 118–122.

Gietz,R.D. and Schiestl,R.H. (1995) Transforming yeast with DNA. *Methods Mol. Cell. Biol.*, **5**, 255–269.

Gonzalez,I., Buonomo,S.B.C., Nasmyth,K. and von Ahsen,U. (1999) *ASH1* mRNA localization in yeast involves multiple secondary structural elements and Ash1 protein translation. *Curr. Biol.*, **9**, 337–340.

Grandi,P., Doye,V. and Hurt,E.C. (1993) Purification of NSP1 reveals complex formation with 'GLFG' nucleoporins and a novel nuclear pore protein NIC96. *EMBO J.*, **12**, 3061–3071.

Haarer,B.K., Petzold,A., Lillie,S.H. and Brown,S.S. (1994) Identification of MYO4, a second class V myosin gene in yeast. *J. Cell Sci.*, **107**, 1055–1064.

Hann,B.C. and Walter,P. (1991) The signal recognition particle in *S.cerevisiae*. *Cell*, **67**, 131–144.

James,P., Halladay,J. and Craig,E.A. (1996) Genomic libraries and a host strain designed for highly efficient two-hybrid selection in yeast. *Genetics*, **144**, 1425–1436.

Jansen,R.-P., Dowzer,C., Michaelis,C., Galova,M. and Nasmyth,K. (1996) Mother cell-specific HO expression in budding yeast depends on the unconventional myosin Myo4p and other cytoplasmic proteins. *Cell*, **84**, 687–697.

Kiebler,M.A. and DesGroseillers,L. (2000) Molecular insights into mRNA transport and local translation in the mammalian nervous system. *Neuron*, **25**, 19–28.

Knop,M., Siegers,K., Pereira,G., Zachariae,W., Winsor,B., Nasmyth,K. and Schiebel,E. (1999) Epitope tagging of yeast genes using a PCR-based strategy: more tags and improved practical routines. *Yeast*, **15**, 963–972.

Lasko,P. (1999) RNA sorting in *Drosophila*. *FASEB J.*, **13**, 421–433.

Long,R.M., Singer,R.H., Meng,X., Gonzalez,I., Nasmyth,K. and Jansen,R.-P. (1997) Mating type switching in yeast controlled by asymmetric localization of *ASH1* mRNA. *Science*, **277**, 383–387.

Mermall,V., Post,P.L. and Mooseker,M.S. (1998) Unconventional myosins in cell movement, membrane traffic and signal transduction. *Science*, **279**, 527–533.

Mowry,K.L. (1999) RNA sorting in *Xenopus* oocytes and embryos. *FASEB J.*, **13**, 435–445.

Mumberg,D., Müller,R. and Funk,M. (1994) Regulatable promoters of *Saccharomyces cerevisiae*: comparison of transcriptional activity and their use for heterologous expression. *Nucleic Acids Res.*, **22**, 5767–5768.

Münchow,S., Sauter,C. and Jansen,R.-P. (1999) Association of the class V myosin Myo4p with a localised messenger RNA in budding yeast depends on She proteins. *J. Cell Sci.*, **112**, 1511–1518.

Nonaka,H., Tanaka,K., Hirano,H., Fujiwara,T., Kohno,H., Umikawa,M. and Mino,A. (1995) A downstream target of *RHO1* small GTP-binding protein is *PKC1*, a homolog of protein kinase C, which leads to activation of the MAP kinase cascade in *Saccharomyces cerevisiae*. *EMBO J.*, **14**, 5931–5938.

Peabody,D.S. (1990) Translational repression by bacteriophage MS2 coat protein expressed from a plasmid. *J. Biol. Chem.*, **265**, 5684–5689.

Query,C.C., Bentley,R.C. and Keene,J.D. (1989) A common RNA recognition motif identified within a defined U1 RNA binding domain of the 70k U1 snRNP protein. *Cell*, **57**, 89–101.

Rothstein,R.J. (1983) One-step gene disruption in yeast. *Methods Enzymol.*, **101**, 202–211.

Schnapp,B.J. (1999) RNA localization: a glimpse of the machinery. *Curr. Biol.*, **9**, R725–R727.

Schnorrer,F., Bohmann,K. and Nuesslein-Volhard,C. (2000) The molecular motor dynein is involved in targeting Swallow and *bicoid* RNA to the anterior pole of *Drosophila* oocytes. *Nature Cell Biol.*, **2**, 185–190.

Schwob,E., Böhm,T., Mendenhall,M.D. and Nasmyth,K. (1994) The B-type cyclin kinase inhibitor p40SIC1 controls the G_1 to S transition in *S.cerevisiae*. *Cell*, **79**, 233–244.

Segref,A., Sharma,K., Doye,V., Hellwig,A., Huber,J., Lührmann,R. and Hurt,E. (1997) Mex67p, a novel factor for nuclear mRNA export,

binds to both poly(A)$^+$ RNA and nuclear pores. *EMBO J.*, **16**, 3256–3271.

Singer,R.H. (1993) RNA zipcodes for cytoplasmic adresses. *Curr. Biol.*, **3**, 719–721.

Solsbacher,J., Maurer,P., Bischoff,F.R. and Schlenstedt,G. (1998) Cse1p is involved in export of yeast importin α from the nucleus. *Mol. Cell. Biol.*, **18**, 6805–6815.

Takizawa,P.A. and Vale,R.D. (2000) The myosin motor, Myo4p, binds Ash1 mRNA via the adapter protein, She3p. *Proc. Natl Acad. Sci. USA*, **97**, 5273–5278.

Takizawa,P.A., Sil,A., Swedlow,J.R., Herskowitz,I. and Vale,R.D. (1997) Actin-dependent localization of an RNA encoding a cell-fate determinant in yeast. *Nature*, **389**, 90–93.

Thio,G.L., Ray,R.P., Barcelo,G. and Schupbach,T. (2000) Localization of gurken RNA in *Drosophila* oogenesis requires elements in the 5′ and 3′ regions of the transcript. *Dev. Biol.*, **221**, 435–446.

Trifillis,P., Day,N. and Kiledjian,M. (1999) Finding the right RNA: identification of cellular mRNA substrates for RNA-binding proteins. *RNA*, **5**, 1071–1082.

Wach,A., Brachat,A., Alberti-Segui,C., Rebischung,C. and Phillippsen,P. (1997) Heterologous *HIS3* marker and GFP reporter modules for PCR-targeting in *Saccharomyces cerevisiae*. *Yeast*, **13**, 1065–1075.

Wendland,B., McCaffery,J.M., Xiao,Q. and Emr,S.D. (1996) A novel fluorescence-activated cell sorter-based screen for yeast endocytosis mutants identifies a yeast homologue of mammalian eps15. *J. Cell Biol.*, **135**, 1485–1500.

Received June 30, 2000; revised August 29, 2000;
accepted August 31, 2000